Pramana – J. Phys., Vol. 39, No. 3, September 1992, pp. 305–316. © Printed in India.

Photoionization of the ground $^1S^e$ and twenty lowest excited states of the Ne-like Fe^{16+}

M MOHAN, M Le DOURNEUF*, VINOD PRASAD and A KUMAR

Department of Physics and Astrophysics, University of Delhi, Delhi 110007, India
Observatoire de Paris, Department "Atomes et molecules in astrophysique", Unite Propre de Recherche n° 261 du CNRS, 92195 Meudon, France

MS received 18 April 1992

Abstract. The R-matrix method is used to calculate cross-sections for the photoionization of Ne-like Fe^{16+} from ground $2s^2 2p^6\,^1S^e$ and excited states belonging to $2s2p^6\ 3l$ and $2s^2 2p^5\ 3l$ configurations. Configuration interaction wavefunctions are used to represent two target states of Fe^{17+} ion retained in the R-matrix expansion. The cross-sections are obtained as a function of kinetic energy (ε_k) of the ejected electron from 10 to 24 Ry. For low kinetic energy the cross-sections show series of Rydberg states which converge onto $^2S^e$ threshold Fe^{17+}. The calculations are carried out in the LS coupling.

Keywords. Photoionization, configuration-interaction; R-matrix method.

PACS No. 34·80

1. Introduction

Recently in the international Atomic Energy Agency meeting (Berrington 1991; Janev 1991), there was an important discussion on the phenomenon related to interaction of electron and photons with ionized atoms, particularly with metallic impurities such as Ti, Cr, Fe and Ni which are important features of controlled thermonuclear plasmas. Further study of neon-like Fe^{17} has also attracted considerable interest in astrophysics as strong emission lines from this have been observed in the solar corona and solar flares (Kastner 1983; Feldman and Doschek 1985; Jupen 1985).

In the present work we have used the R-matrix method of Burke and Taylor (1975) to obtain accurate photoionization cross-section from the ground $2p^6\,^1S^e$ and twenty lowest excited states belonging to $2s2p^6\ 3l$ and $2s^2 2p^5\ 3l$ configurations. Here the initial bound state of Fe^{16+} and final continuum states constructed from residual ion Fe^{17+} plus an outgoing electron are expanded consistently on collision type R-matrix basis set expressed in terms of states of N-electron residual ion Fe^{17+}. We assume here that the residual ion is left in the two lowest states $2s^2 2p^5\ 2p^0$ and $2s2p^6\,^2S^e$. For the target states we use the configuration interaction (CI) wavefunction as described by Mohan and Hibbert (1991) and used sucessfully by Mohan *et al* (1990, 1991) in the calculation of accurate collision strengths for electron impact excitation of positive ions.

A point worth mentioning here is that this is the first detailed calculation on photoionization of ground and excited states of Fe^{16+} where all the important physical

effects like exchange, channel coupling and short range correlations are taken into account.

2. Calculations

In the present work, we have calculated the photoionization cross-section of the ground $2s^2 2p^6\,{}^1S^e$ and excited $2s2p^6 3s\,{}^{1,3}S$, $2s2p^6 3p$, ${}^{1,3}P^0$, ${}^{1,3}D^0$, $2s^2 2p^5 3d$, ${}^{1,3}P^0$, ${}^{1,3}D^0$, ${}^{1,3}F^0$ states of Fe^{16+} as a function of kinetic energy ε_k of the ejected electron from 10 to 24 Ry which corresponds to photon energy lying just above $2s2p^6\,{}^2S^e$ threshold of target ion Fe^{17+}. At these energies, only the channels associated to first two ${}^2P^0$ and ${}^2S^e$ states of Fe^{17+} are open, therefore photoionization process which we studied from ground ${}^1S^e$ and any excited state e.g. from next excited state ${}^3P^0$ can be represented as follows:

$$\begin{aligned} h\nu + \mathrm{Fe}^{16+}(2s^2 2p^6\,{}^1S) &\rightarrow \mathrm{Fe}^{17+}(2s^2 2p^5\,{}^2P^0) + e^-, \\ &\rightarrow \mathrm{Fe}^{17+}(2s2p^6\,{}^2S) + e^-, \qquad (1) \\ h\nu + \mathrm{Fe}^{16+}(2s^2 2p^6\,{}^3P^0) &\rightarrow \mathrm{Fe}^{17+}(2s^2 2p^5\,{}^2P^0) + e^-, \\ &\rightarrow \mathrm{Fe}^{17+}(2s2p^6\,{}^2S) + e^-. \qquad (2) \end{aligned}$$

2.1 *Target wavefunction*

The configuration interaction wavefunctions for Fe^{17+} have recently been obtained by Mohan and Hibbert (1991) using CIV3 code (Hibbert 1975). In LS coupling these wavefunctions can be represented by CI expansions of the form

$$\Psi(\mathrm{LS}) = \sum_{i=1}^{N} a_i \Phi_i(\alpha_i \mathrm{LS}), \qquad (3)$$

where $\{\Phi_i\}$ represent single configuration functions in which the orbital and spin angular momentum of the electrons are coupled (as specified by $\{\alpha_i\}$) to form a total L and S common to all M configurations. The radial part of each orbital is written in analytic form as a sum of Slater type orbitals

$$P_{nl}(r) = \sum_{i=1}^{k} C_i r^{p_i} \exp(-\tau_i r). \qquad (4)$$

The parameters $\{c_i\}$ $\{p_i\}$ and $\{\tau_i\}$ in (4) are determined variationally as described by Mohan and Hibbert (1991). In this calculation six orthogonal one electron orbitals $1s, 2s, 2p, 3s, 3p, 3d$ are used. The radial functions for the $1s, 2s$ and $2p$ orbitals were those of ground state, given by Clementi and Roeti (1974), while those for $3s, 3p, 3d$ orbitals were optimized using CIV3 on the excited states $2p^4\,({}^1D)3s\,{}^2D, 2p^4({}^3P)3p\,{}^2D^0$ and $2p^4(3p)\,3d\,{}^2F$ respectively. In table 1 we have given the parameters for $3s$, $3p$ and $3d$ orbitals where $3s$ and $3p$ are determined uniquely as described by Mohan *et al* (1991). In table 2 we have given the configuration used in the CI expansion of the target states $2s^2 2p^5\,{}^2P^0$ and $2s2p^6\,{}^2S$ included in the calculations while in table 3 we have listed the experimental and theoretical energy separations. The agreement between the experimental and theoretical energy separations is reasonably good. The

Table 1. Parameters of $3l$ Slater-type orbitals.

Orbitals	P_i	τ_i
$3s$	1	18·99771
	2	8·36074
	3	6·51914
$3p$	2	10·62696
	3	6·03611
$3d$	3	8·45703
	3	5·86267
$3d$ coefficients	c_i	
	0·05793	
	0·97374	

Table 2. Configuration used in the CI expansion of Fe^{17+} target state.

State		Configuration used
$[1s^2]2s^22p^5$	$^2p^0$	$1s^22s^22p^5, 2s^22p^4(^3p)3p, 2s^22p^4(^1S)3p,$ $2p^5(^2P)3s^2, 2p^5(^2P)3p^2, 2s^22p^4(^1D)3p$
$2s2p^6$	^2S	$2s2p^6, 2s2p^5(^3P)3p, 2s2p^5(^1P)3p,$ $2s^22p^4(^1S)3s, 2p^6(^1S)3s, 2s^22p^4(^1D)3d$

Table 3. Excitation threshold for Fe^{17+}.

	Energy (Ry)	
Configuration state	Theor.	Expt.
$1s^22s^22p^5\,2P^0$	0	0
$1s^22s2p^6\,^2S^e$	8·67334	8·76590

difference is mainly due to the omission of mass correction and Darwin term from the calculation.

2.2 *The $(N+1)$-electron system wavefunction*

The initial and final continuum wavefunctions used for the photoionization of an $(N+1)$ electron system are expanded in the inner configuration space $r \leqslant a$, as described by Burke and Robb (1975), in terms of discrete R-matrix basis function of adequate LS symmetry as

$$\Psi_k^{LS\pi} = A \sum_{ij} C_{ijk} \Phi_i^{LS\pi}(x_1, x_2, \ldots\ldots x_N, \hat{r}_{N+1}\sigma_{N+1}) U_{ij}(r_{N+1})$$

$$+ \sum_j d_{jk} \Psi_j(x_i, \ldots\ldots, x_{N+1}), \tag{5}$$

where A is the antisymmetrization operator which accounts for the electron exchange, Φ_i are channel functions formed by coupling the target states Φ_i to the orbital and spin angular momenta of the scattering channel, U_{ij} are the continuum basis orbitals

and Φ_j are the $(N+1)$-electron bound configurations which account both for the short range correlation effects and also make some allowance for the omitted channels in the first expansion. The Ψ_j are square integrable functions consisting of $(N+1)$ electron configurations. The coefficients c_{ijk} and d_{jk} as well as the corresponding eigenvalues, are determined by diagonalising the $(N+1)$ electron Hamiltonian in the internal region. The continuum orbitals U_{ij} in (5) are solutions of the radial differential equation

$$[(\mathrm{d}^2/\mathrm{d}r^2 - l_i(l_i+1)/r^2 + V(r) + k_i^2]\,U_{ij}(r) = \sum_k \lambda_{ijk} P_{kl}(r) \tag{6}$$

satisfying the boundary conditions

$$U_{ij}(0) = 0 \tag{7}$$

and

$$(a/U_{ij})(d\,U_{ij}/\mathrm{d}r)|_{r=2} = b \tag{8}$$

derivative ($b = 0$) on the continuum basis orbitals. In (6) $|l_i$ is the angular momentum of the scattered electron, $V(r)$ is the static potential of the target in its ground state and λ_{ijk} are Langrange multipliers which are determined in order to impose the orthogonality of the continuum orbitals to bound radial orbitals $P_k(r)$ having the same angular momentum l_i. We imposed a zero logarithmic derivative ($b = 0$) at the R-matrix boundary radius $a = 3{\cdot}40$ a.u. and we retained 15 continuum orbitals for each angular symmetry, to ensure convergence in the energy range considered.

3. Results and discussion

The cross-section for the photoionization of the $2s^2 2p^6\,{}^1S^e$ ground state and 20 lowest excited states are obtained in the LS coupling. The energy region of interest is the resonance region close to the ionization threshold and below 24 Ry free electron energy.

3.1 *Photoionization from* $^1S^e$ *states*

The direct photoionization of $^1S^e$ ground state can be represented by

$$\mathrm{Fe}^{16+}(2s^2 2p^6\,{}^1S^e) + h\nu \rightarrow \mathrm{Fe}^{17+}(2s^2 2p^5\,{}^2P^0) + e^-(ks, kd). \tag{9}$$

The process leading to the enhancement of direct photoionization by excitation and autoionization to the continuum is expressed as

$$\mathrm{Fe}^{16+}(2s^2 2p^6\,{}^1S^e) + h\nu \rightarrow \mathrm{Fe}^{16+}(2s^2 2p^5 nl\,{}^1P^0) \tag{10}$$

$$\rightarrow \mathrm{Fe}^{17+}(2s^2 2p^5\,{}^2P^0) + e^- \tag{11}$$

$$\rightarrow \mathrm{Fe}^{17+}(2s2p^6\,{}^2S^e) + e^-. \tag{12}$$

The above process can only take place at the energy above the $^2S^e$ ionization threshold of Fe^{17+} at photon energy 8·673 Ry.

In figure 1 we have plotted the photoionization cross-section of the $^1S^e$ ground

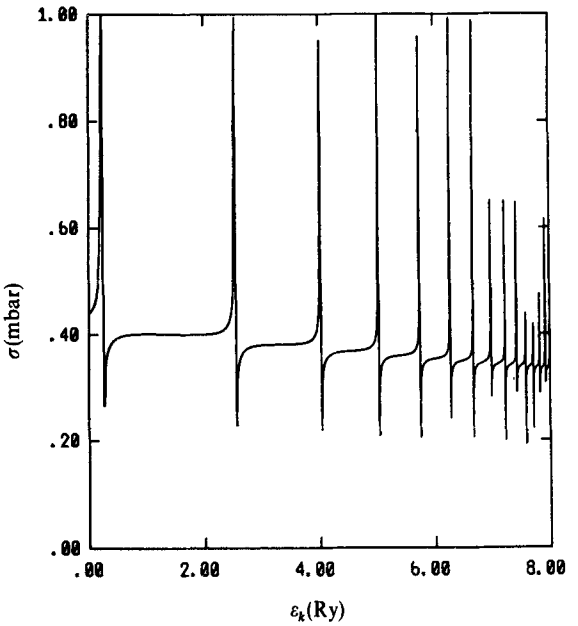

Figure 1. Total photoionization cross-section in mbar for the ground state $[1s^2]2s^2 2p^6\,{}^1S^e$ of Fe^{16+} below the $^2S^e$ threshold plotted as a function of photoelectron energy in Rydberg.

state as a function of the photoelectron energy in Rydberg (where photon energy = ionization potential (IP) + photoelectron energy) in the energy range from $^2P^0$ threshold to just near the $^2S^e$ threshold of Fe^{17+}. This energy region is dominated by closed channel (or Feshbach) resonances which perturb the otherwise smoothly varying background cross-section. These resonances belong to the $2s2p^6\,{}^2S^e$ np Rydberg series and converge on to the $^2S^e$ threshold. This process can be represented by

$$h\nu + Fe^{16+}(2s^2 2p^6\,{}^1S^e) \rightarrow Fe^{17+}(2s2p^6\,{}^2S^e np)\,{}^1P^0$$

which clearly corresponds to jump from $2s$ to $2p$ from the inner shell. In the energy above the $^2S^e$ threshold we have smoothly varied background up to 35 Ry as the next higher state $2s^2 2p^4(3p)3s\,{}^4P$ lies quite beyond $^2S^e$ and has a threshold at 56·93 Ry. In the first column of table 4 we have given the photoionization cross-section σ in mbar for photoionization from the $^1S^e$ ground state for photoelectronic energy from 10 to 24 Ry.

In figures 2 and 3 we have plotted the photoionization cross-sections from the next higher states $2s^2 2p^5 3p$ and $2s2p^6 3s$ belonging to $^1S^e$ symmetries. Here like the ground state $^1S^e$, we find one set of Rydberg series belonging to $^2s2p^6\,{}^2S^e$ np configurations. In the second and third columns of table 5 under $^1S^e$ heading we have given the photoionization cross-section from those states for the photoelectron energies from 10 to 24 Ry.

3.2 *Photoionization from $^3P^0$ states*

The direct photoionization of the next excited state of Fe^{16+} can be written as

$$h\nu + Fe^{16+}(2s^2 2p^5 3s^3 P^0) \rightarrow Fe^{17+}(2s^2 2p^5\,{}^2P^0) + e^-. \qquad (13)$$

Table 4. Ground and 20 excited states of Fe^{16+} belonging to different symmetries.

Symmetry	States
$^1S^e$	$[1s^2]2s^22p^6, 2s^22p^5(^2p^0)3p, 2s2p^63s$
$^3P^0$	$2s^22p^53s, 2s^22p^53d, 2s2p^63p$
$^1P^0$	$2s^22p^53s, 2s^22p^53d, 2s2p^63p$
$^3S^e$	$2s^22p^53p, 2s2p^63s$
$^3D^e$	$2s^22p^53p, 2s2p^63d$
$^1D^e$	$2s^22p^53p, 2s2p^63d$
$^1P^e$	$2s^22p^53p$
$^3P^e$	$2s^22p^53p$
$^3F^0$	$2s^22p^53d$
$^1F^0$	$2s^22p^53d$
$^3D^0$	$2s^22p^53d$
$^1D^0$	$2s^22p^53d$

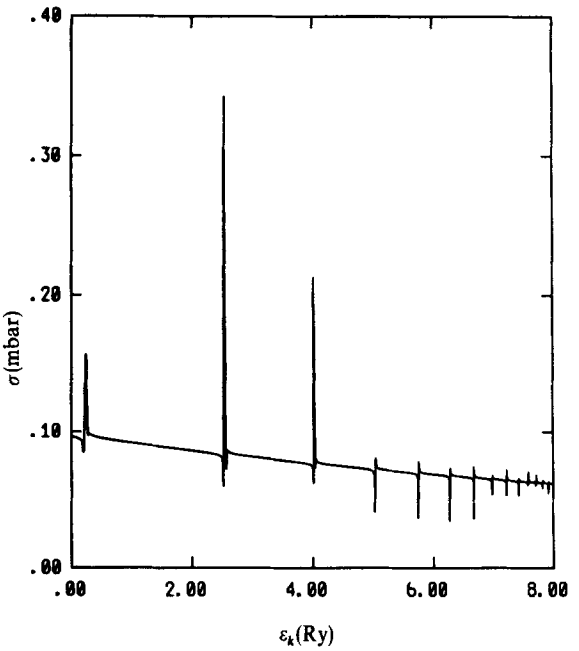

Figure 2. Same as in figure 1, but from $[1s^2]2s^22p^53p\,^1S^e$ state.

The $^3P^e$, $^3D^e$ and $^3S^e$ final states are allowed by dipole selection rule for photoionization from this state. The total photoionization is obtained by summing over the contributions of these final states and the process can be written as

$$h\nu + Fe^{16+}(2s2p^53s\,^3P^0) \rightarrow Fe^{16+}(2s^22p^5nl\,^3D^e, {}^3P^e, {}^3S^e), \tag{14}$$

$$\rightarrow [Fe^{17+}(2s^22p^5\,^2P^0 + e^-)^3D^e, {}^3P^e, {}^3S^e, \tag{15}$$

$$\rightarrow [Fe^{17+}(2s2p^6\,^2S^e + e^-)^3D^e, {}^3S^e. \tag{16}$$

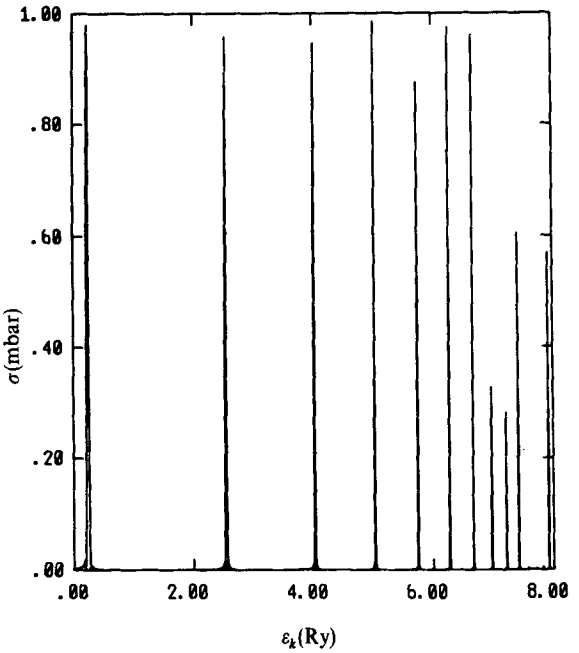

Figure 3. Same as in figure 1, but from $[1s^2]2s2p^6 3s^1S^e$ state.

Table 5. Total photoionisation cross-section of Fe^{17} in (MB) from various LS levels.

1SE			
Symmetry =	1	2	3
I.P(Ry) =	−92·7351	−35·0539	−29·7833
Ekin(Ry)	CROS. (MB)	CROS. (MB)	CROS. (MB)
0·100000E + 02	0·38234E + 00	0·56018E − 01	0·59729E − 01
0·120000E + 02	0·36444E + 00	0·50773E − 01	0·54754E − 01
0·140000E + 02	0·34775E + 00	0·46289E − 01	0·50299E − 01
0·160000E + 02	0·33242E + 00	0·42418E − 01	0·46353E − 01
0·180000E + 02	0·31829E + 00	0·39029E − 01	0·42914E − 01
0·200000E + 02	0·30505E + 00	0·36022E − 01	0·39968E − 01
0·220000E + 02	0·29238E + 00	0·33337E − 01	0·37497E − 01
0·240000E + 02	0·28016E + 00	0·30971E − 01	0·35482E − 01
3PO			
Symmetry =	1	2	3
I.P(Ry) =	−39·1335	−33·7995	−27·8563
Ekin(Ry)	CROS. (MB)	CROS. (MB)	CROS. (MB)
0·100000E + 02	0·40937E − 01	0·39366E − 01	0·83418E − 01
0·120000E + 02	0·38113E − 01	0·34067E − 01	0·74556E − 01
0·140000E + 02	0·35646E − 01	0·29570E − 01	0·66864E − 01
0·160000E + 02	0·33488E − 01	0·25774E − 01	0·60152E − 01
0·180000E + 02	0·31594E − 01	0·22587E − 01	0·54258E − 01
0·200000E + 02	0·29944E − 01	0·19921E − 01	0·49043E − 01
0·220000E + 02	0·28580E − 01	0·17691E − 01	0·44392E − 01
0·240000E + 02	0·27790E − 01	0·15822E − 01	0·40249E − 01

(*Continued*)

Table 5. (*Continued*)

1PO					
Symmetry =	1	2	3		
I.P(Ry) =	−38·9025	−32·5111	−27·6734		
Ekin(Ry)	CROS. (MB)	CROS. (MB)	CROS. (MB)		
0·100000E + 02	0·40887E − 01	0·32258E − 01	0·83640E − 01		
0·120000E + 02	0·38081E − 01	0·27612E − 01	0·74885E − 01		
0·140000E + 02	0·35655E − 01	0·23493E − 01	0·67292E − 01		
0·160000E + 02	0·33568E − 01	0·20080E − 01	0·60667E − 01		
0·180000E + 02	0·31787E − 01	0·17249E − 01	0·54852E − 01		
0·200000E + 02	0·30320E − 01	0·14898E − 01	0·49719E − 01		
0·220000E + 02	0·29291E − 01	0·12943E − 01	0·45173E − 01		
0.240000E + 02	0·29282E − 01	0·11313E − 01	0·41192E − 01		
3SE			3DE		
Symmetry =	1	2	Symmetry =	1	2
I.P(Ry) =	−37·2001	−30·2289	I.P(Ry) =	−36·7747	−24·7961
Ekin(Ry)	CROS. (MB)	CROS. (MB)	Ekin(Ry)	CROS. (MB)	CROS. (MB)
0·100000E + 02	0·55432E − 01	0·59918E − 01	0·100000E + 02	0·53721E − 01	0·68040E − 01
0·120000E + 02	0·50683E − 01	0·55007E − 01	0·120000E + 02	0·48954E − 01	0·56566E − 01
0·140000E + 02	0·46478E − 01	0·50628E − 01	0·140000E + 02	0·44735E − 01	0·47448E − 01
0·160000E + 02	0·42745E − 01	0·46748E − 01	0·160000E + 02	0·40987E − 01	0·40019E − 01
0·180000E + 02	0·39421E − 01	0·43346E − 01	0·180000E + 02	0·37645E − 01	0·33819E − 01
0·200000E + 02	0·36457E − 01	0·40400E − 01	0·200000E + 02	0·34658E − 01	0·28553E − 01
0·220000E + 02	0·33844E − 01	0·37863E − 01	0·220000E + 02	0·31993E − 01	0·24035E − 01
0·240000E + 02	0·31868E − 01	0·35557E − 01	0·240000E + 02	0·29727E − 01	0·20148E − 01
1DE			1PE		
Symmetry =	1	2	Symmetry =	1	
I.P(Ry) =	−36·5884	−24·3964	I.P(Ry) =	−36·5506	
Ekin(Ry)	CROS. (MB)	CROS. (MB)	Ekin(Ry)	CROS. (MB)	
0·100000E + 02	0·53503E − 01	0·64705E − 01	0·100000E + 02	0·53530E − 01	
0·120000E + 02	0·48725E − 01	0·53564E − 01	0·120000E + 02	0·48824E − 01	
0·140000E + 02	0·44506E − 01	0·44760E − 01	0·140000E + 02	0·44655E − 01	
0·160000E + 02	0·40765E − 01	0·37630E − 01	0·160000E + 02	0·40949E − 01	
0·180000E + 02	0·37431E − 01	0·31722E − 01	0·180000E + 02	0·37642E − 01	
0·200000E + 02	0·34446E − 01	0·26743E − 01	0·200000E + 02	0·34680E − 01	
0·220000E + 02	0·31767E − 01	0·22511E − 01	0·220000E + 02	0·32021E − 01	
0·240000E + 02	0·29364E − 01	0·18901E − 01	0·240000E + 02	0·29631E − 01	
3PE			3FO		
Symmetry =	1		Symmetry =	1	
I.P(Ry) =	−36·5433		I.P(Ry) =	−33·6052	
Ekin(Ry)	CROS. (MB)		Ekin(Ry)	CROS. (MB)	
0·100000E + 02	0·54451E − 01		0·100000E + 02	0·35689E − 01	
0·120000E + 02	0·49614E − 01		0·120000E + 02	0·30743E − 01	
0·140000E + 02	0·45339E − 01		0·140000E + 02	0·26553E − 01	
0·160000E + 02	0·41543E − 01		0·160000E + 02	0·23022E − 01	
0·180000E + 02	0·38158E − 01		0·180000E + 02	0·20066E − 01	
0·200000E + 02	0·35130E − 01		0·200000E + 02	0·17604E − 01	
0·220000E + 02	0·32427E − 01		0·220000E + 02	0·15552E − 01	
0·240000E + 02	0·30132E − 01		0·240000E + 02	0·13830E − 01	

(*Continued*)

Table 5. (*Continued*)

1FO		3DO	
Symmetry =	1	Symmetry =	1
I.P(Ry) =	−33·3929	I.P(Ry) =	−33·3062
Ekin(Ry)	CROS. (MB)	Ekin(Ry)	CROS. (MB)
0·100000E + 02	0·34224E − 01	0·100000E + 02	0·35799E − 01
0·120000E + 02	0·29434E − 01	0·120000E + 02	0·30828E − 01
0·140000E + 02	0·25392E − 01	0·140000E + 02	0·26624E − 01
0·160000E + 02	0·21993E − 01	0·160000E + 02	0·23083E − 01
0·180000E + 02	0·19154E − 01	0·180000E + 02	0·20120E − 01
0·200000E + 02	0·16793E − 01	0·200000E + 02	0·17652E − 01
0·220000E + 02	0·14829E − 01	0·220000E + 02	0·15595E − 01
0·240000E + 02	0·13185E − 01	0·240000E + 02	0·13869E − 01
1DO			
Symmetry =	1		
I.P(Ry) =	−33·3087		
Ekin(Ry)	CROS. (MB)		
0·100000E + 02	0·35775E − 01		
0·120000E + 02	0·30815E − 01		
0·140000E + 02	0·26619E − 01		
0·160000E + 02	0·23087E − 01		
0·180000E + 02	0·20133E − 01		
0·200000E + 02	0·17674E − 01		
0·220000E + 02	0·15627E − 01		
0·240000E + 02	0·13913E − 01		

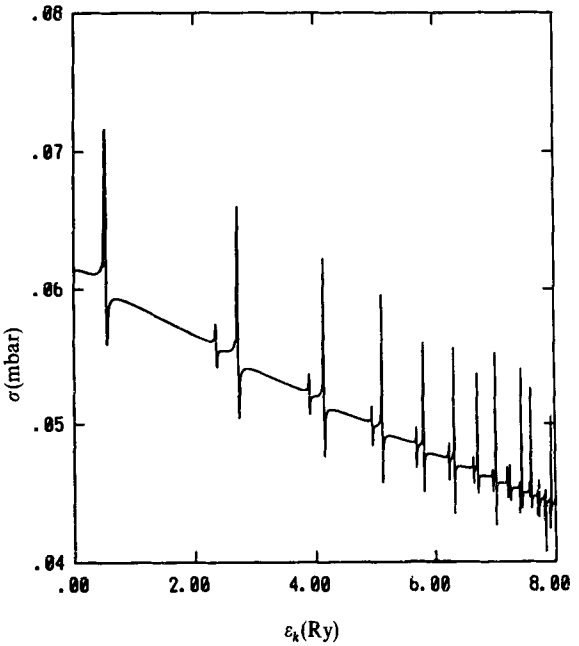

Figure 4. Same as in figure 1, but from $[1s^2]2s^22p^53s^3P^0$ state.

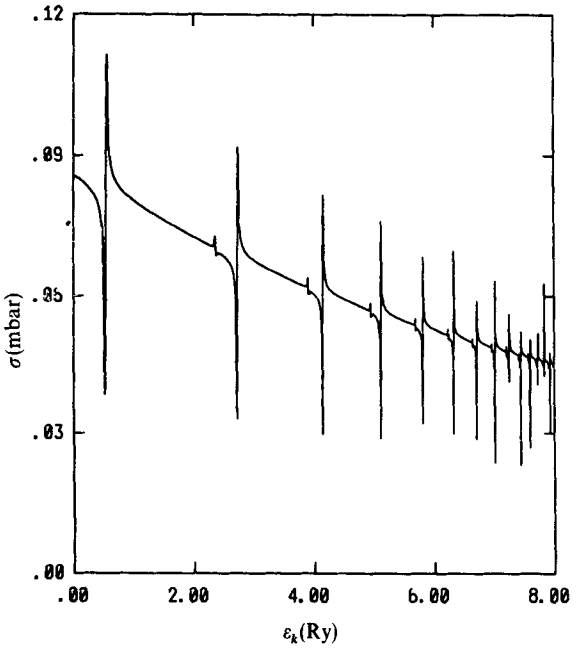

Figure 5. Same as in figure 1, but from $[1s^2]2s^22p^53d^3P^0$ state.

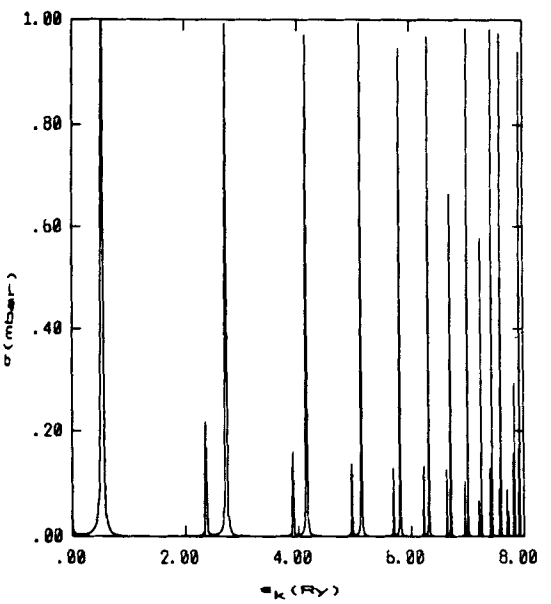

Figure 6. Same as in figure 1, but from $[1s^2]2s2p^63p^3P^0$ state.

It is to be noted that the final $^3P^e$ state does not couple to the $^2S^e$ excited state of Fe^{17+} and therefore does not lead to any further increase in the cross-section. In figure 4 we have plotted the total photoionization cross-section from this state in mbar for photoelectron energy from near to $2s2p^6\,^2S^e$ threshold of Fe^{17+}. Here as expected

we find two Rydberg series $[Fe^{17+}(2s2p^6\,^2S^e)ns]\ ^3S^e$ and $[Fe^{17+}(2s2p^6\,^2S^e)nd]$ converging to $^2S^e$ threshold. Similarly in figures 5 and 6 we have shown the photoionization cross-section from next excited states $2s^22p^5$ and $2s2p^63p$ beloning to $^3P^0$ symmetry which also shows two sets of the Rydberg *ns* and *nd* series. In table 4 under the $^3P^0$ symmetry heading we have given the cross-sections for $2s2p^53s, ^3P^0$, $2s^22p^53d, ^3P^0$ and $\angle s2p^63p\,^3P^0$ states for the photoelectron energy from 10 to 24 Ry.

3.3 *Photoionization of other excited states with symmetry* $^1P^0, ^3S^e, ^3D^e, ^1D^e, ^1P^e, ^3P^e, ^3F^0, ^1F^0, ^3D^0, ^1D^0$

We have seen from above that photoionization cross-section from various states of Fe^{16+} vary continuously up to the $2S^e$ threshold due to Feshbach resonances which makes it difficult to tabulate these for photon energy up to 8·67 Ry. For comparision with any future calculations or experiment we have given in table 5 the cross-sections for all these states for the photoelectron energy from 10 to 24 Ry. (However, the results up to $^2S^e$ threshold can be obtained from the authors on request). In table 4 we have given the states corresponding to various symmetries from which photoionization cross-section is calculated.

As can be seen from table 5 the cross-section for photoionization from the ground state is maximum due to the largest oscillator strength for dipole allowed $^1S^e \rightarrow {}^1P^0$ transition for Fe^{16+} (Hibbert *et al* 1992). Further it can be seen that the photoionization from the same configurations states e.g. $2s^22p^53p$ with different symmetries like $^1D^e$ and $^3D^e$ are quite close to each other. This is because they are coupled to similar partial waves with similar angular momentum e.g. here $l = 1$, 2 and 3.

4. Conclusion

In this work the initial and final states are represented consistently by the *R*-matrix expansions over the two ionic states $^2P^0$ and $^2S^e$ which are described by sophisticated configuration interaction wavefunction. At low energy the cross-sections are found to be dominated by closed channel Feshbach resonances.

We expect our results to be quite reliable, as we have taken all the important physical effects like exchange, channel coupling and short range correlation into account.

Acknowledgements

The authors are thankful to the 'Indo-French Centre for the Promotion of Advanced Research' for financial support. One of the authors (MM) is also thankful to DST and UGC for financial support.

References

Berrington K A 1991 *Phys. Scr.* **37** 19
Burke P G and Robb W D 1975 *Adv. At. Mol. Phys.* **11** 143
Burke P G and Taylor P G 1975 *J. Phys.* **B8** 2620

Feldman U and Doschek G A J F 1985 *Mon. Not. R. Astron. Soc.* **212** 41
Hibbert A 1975 *Comput. Phys. Commun.* **9** 141
Hibbert A, Dourneuf M Le and Mohan M 1992 Energy levels and weighted oscillator strengths of neon isoelectronic sequence. *At. Data Nucl. Data Tables* (communicated)
Janev R K 1991 *Phys. Scr.* **T37** 5
Jupen C 1985 *Mon. Not. R. Astron. Soc.* **208** 1
Kastner S O 1983 *Astrophys. J.* **275** 922
Mohan M and Hibbert A 1991 *Phys. Scr.* **44** 158
Mohan M and Dourneuf M Le 1990a *Astron. Astrophys.* **22** 285
Mohan M and Dourneuf M Le 1990b *Phys. Rev.* **A41** 2862
Mohan M, Hibbert A and Burke P G 1990a *J. Phys.* **B23** 997
Mohan M, Hibbert A, Berrington K A and Burke P G 1990b *J. Phys.* **B23** 989
Mohan M, Dourneuf M Le, Hibbert A and Burke P G 1990c *Mon. Not. R. Astron. Soc.* **243** 372
Mohan M, Hibbert A and Burke P G 1991a *J. Phys.* **B24** 299
Mohan M, Baliyan K S and Hibbert A 1991b *J. Phys.* **B24** 4159